Int. J. Electrochem. Sci., 12 **(2017)** 1106 – 1117, doi: 10.20964/2017.02.43

International Journal of
ELECTROCHEMICAL
SCIENCE
www.electrochemsci.org

Influence of Chloride on Passive Film Chemistry of 304 Stainless Steel in Sulphuric Acid Solution by Glow Discharge Optical Emission Spectrometry Analysis

Saifu Deng, Shuangbao Wang[*]*, Linyue Wang, Jianting Liu, Yujie Wang*

School of Optics and Electronic Information, Huazhong University of Science & Technology, Wuhan 430074, China
[*]E-mail: shuangbaowang@126.com

Received: 14 November 2016 / *Accepted:* 19 December 2016 / *Published:* 30 December 2016

The influence of chloride on passive film formed on 304 stainless steels (SS) in 0.2 M H_2SO_4 solution has been investigated by potentiostatic polarization experiments and glow discharge optical emission spectroscopy (GD-OES) analysis. Chromium was enriched in outer and inner layers of passive film after potentiostatic passivation. The Cr/Fe ratio of the passive film increased with immersion time of passivation, which suggested the improvement of corrosion resistance. The breakdown of passivity was evaluated by addition of sodium chloride (NaCl). Pitting corrosion appeared on the surface of the passive film when 3 wt% of NaCl was added into the solution, thereby resulting in a decrease of iron species in the outer layer of the passive film. The depth profiles showed the appearance of chlorine in the passive film region of 304 SS polarized in chloride-containing solution. The decrease of Cl species intensity from the outer layer to the inner layer validated the penetration of chloride ions through passive film during pitting corrosion.

Keywords: 304 stainless steel, GD-OES, passive film, pitting corrosion.

1. INTRODUCTION

Stainless steel (SS) can be easily transformed into passive state in the presence of a small amount of oxidizing agent in solution [1]. Varge et al. [2, 3] studied the adsorption behavior of SO_4^{2-} ions by radiotracer method. They found that a link between the formation of Cr^{3+} species in the passive film and SO_4^{2-} adsorption can be formulated. However, the Cl ion additives in the solution would lead to the breakdown of passivity and initiation of pitting corrosion [4]. The polarization behavior in Cl^- ion-containing solution has been investigated for decades [5–11]. For example, Lee et al. [11] studied

the effects of sulphuric ion additives on the pitting corrosion of pure aluminum in sodium chloride (NaCl) solution. They suggested that SO_4^{2-} ions retard the oxide film breakdown by Cl^- ion incorporation into the film, which revealed the competitive adsorption between Cl^- ions and $SO4^{2-}$ ions.

Many studies [12–15] have been performed on the effect of chloride on the passivity and transpassivation behavior. The passivity breakdown of 304 stainless steel is attributed to the formation of chloride in passive film and highly charged chromium ions (mostly Cr^{6+} species). Rao et al. [16] studied the corrosion behavior and chemical structure of the passive film of 216 L SS in sulfuric acid. In this study, the enrichment of Cr ions on the surface is revealed from the XPS results, but the breakdown mechanism caused by Cl^- ions remains unclear. Saadi et al. [17] found that the chlorine ion intensities at the film/metal interface were correlated with the ending potential of potentiodynamic polarization, which supported the passivity breakdown mechanisms, considering the role of chlorine ions at the metal/film interface instead of film/solution interface. However, the main concern is the mechanism of passivity breakdown. Moreover, the passive film chemistry of stainless steel needs further investigation.

To examine the elemental depth profiles of surface film, various surface analytic techniques have been used, such as X-ray photoelectron spectroscopy (XPS), Auger electron spectroscopy, secondary ion mass spectrometry, and glow discharge optical emission spectroscopy (GD-OES) [18–23]. By contrast, GD-OES shows a greater advantage in rapid detection and convenient operation because of its high sputtering rate (over than 1 μm/min). Obtaining the depth profiles of passive film using XPS analysis takes several hours [22]. However, this amount of time can be reduced to within a few seconds by GD-OES [23]. Owing to the high efficiency of measurement, not only extreme thin film (less than 10 nm), but also relatively thick coating (more than 100 μm) can be analyzed [24–27].

In this work, GD-OES was used to investigate the influence of chloride on the passive film chemistry of 304 SS in H_2SO_4 solution. Potentiodynamic polarization testing was performed in H_2SO_4 solution, thereby containing different concentrations of NaCl. The effect of chloride on the chemical composition of the passive film formed on 304 SS after potentiostatic passivation was discussed.

2. EXPERIMENTAL

2.1 Material and sample preparation

AISI type 304 SS was used in this study, and its chemical compositions are shown in Table 1. Specimens with size of 30 mm × 30 mm × 2 mm were cut from the 304 SS plate, and sample surfaces were ground up to #3000 using SiC papers and polished with 0.5 μm diamond slurry, and then ultrasonically cleaned and dried before they were introduced into the electrochemical cell.

2.2 Potentiodynamic polarization testing

Potentiodynamic polarization was performed with a convectional three-electrode set-up. An area of 10 mm^2 × 10 mm^2 was exposed as working electrode, and a platinum foil and a saturated calomel electrode (SCE) were used as counter electrode and reference electrode, respectively. Before

the polarization, samples were cathodically polarized at −700 mV for 5 min to remove air-formed surface oxide. Then, they were polarized from the cathodic treatment potential in the positive direction at a scan rate of 1 mV/s. The tests were performed in 0.2 M H_2SO_4 solution, thereby containing different contents (0, 1, 2, and 3 wt%) of sodium chloride. All the tests were conducted at 20±2 °C.

2.3 Potentiostatic polarization experiments

The 304 SS were potentiostatically polarized at 0.4 V (vs. SCE) in 0.2 M H_2SO_4 solution for 2 h to generate a dense passive film, which is investigated in this study. To discuss the effect of Cl^- ions on the passive film of 304 SS, different contents (1 and 3 wt%) of NaCl were added into the present electrochemical cell to evaluate the alteration of polarization status while the potential remained unchanged.

2.4 Depth profile analysis

Elemental depth distributions were obtained by glow discharge optical emission spectrometry using a GD-Profiler 2 (Jobin-Yvon) instrument operating in an argon atmosphere of 700 Pa with application of RF of 13.56 MHz and power of 35 W. A 4 mm-diameter copper anode and high-purity argon gas were used. The emission lines used were 425.43 nm (Cr), 371.99 nm (Fe), 341.48 nm (Ni), 130.22 nm (O), and 134.72 nm (Cl). Light emissions of characteristic wavelengths were monitored throughout the analysis with a sampling time of 1 ms to obtain depth profiles. The depth profiles were also examined by a Kratos Axis Ultra X-ray photo-electron spectrometer. Overview spectra were recorded from 200 to 1000 eV kinetic energies with a step size of 1 eV. The binding energy accuracy was calibrated with respect to the C 1s signal at 285 eV. The depth profiles were obtained from every 30 s.

Table 1. Chemical composition of AISI type 304 SS.

Type	Fe	Cr	Ni	Si
wt%	72.36	18.61	08.26	00.76
at%	71.14	19.65	07.73	01.48

3. RESULTS AND DISCUSSION

3.1 Potentiodynamic polarization responses

The potentiodynamic polarization curves of 304 SS in 0.2 M H_2SO_4 containing different concentrations of NaCl are shown in Figure 1. The nature of polarization curves of both the alloys appeared to be similar and all the specimens showed a typical anodic polarization behavior consisting

of passivity and transpassivation (a rapid increase in the current density) [28]. A wide passive range was observed from the figure in H_2SO_4 solution without chloride content, which suggested strong corrosion resistance.

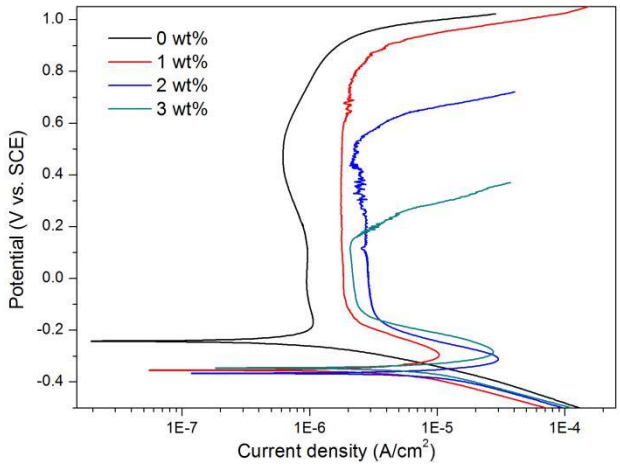

Figure 1. Potentiodynamic polarization curves of 304 SS in 0.2 M H_2SO_4 containing different concentrations of NaCl: (a) 0 wt%, (b) 1 wt%, (c) 2 wt%, and (d) 3 wt%.

Table 2. Electrochemical parameters obtained from potentiodynamic polarization curves.

Content (wt%)	E_{corr} (V vs. SCE)	i_{corr} ($\mu A/cm^2$)	i_{crit} ($\mu A/cm^2$)	E_{pass} (V vs. SCE)	i_{pass} ($\mu A/cm^2$)	E_{pit} (V vs. SCE)
0	-0.243	0.99	1.07	-0.178	0.94	0.932
1	-0.355	11.43	10.23	-0.290	1.78	0.897
2	-0.367	14.86	30.39	-0.309	2.82	0.607
3	-0.347	13.72	27.79	-0.283	2.16	0.145

E_{corr} and i_{corr} are respectively corrosion potential and corrosion current density. I_{crit} is critical current density. i_{pass} and E_{pass} are respectively passive current density and passive potential. E_{pit} is pitting potential

The electrochemical parameters calculated from the curves were tabulated in Table 2. The icorr values were obtained by extrapolating the fitting lines of the anodic and cathodic branch. The value of E_{pit} was taken from the point of intersection between the fitting line of passivation and transpassivation [29]. A decrease of E_{corr} from −0.24 to approximately −0.35 V in chloride-containing solution suggested the weakness of corrosion resistance caused by Cl^- ions, but the E_{corr} value was similar in the presence of different concentrations of chloride additives. The value of i_{corr} increased by one order of magnitude compared with that of the H_2SO_4 solution without chloride content, and the i_{pass} value underwent the same changes. The passive potential (E_{pass}) decreased with the concentration of chloride additives, but no significant change was found.

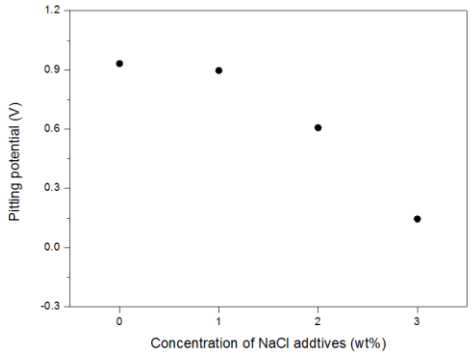

Figure 2. Relationship between pitting potential during potentiodynamic polarization and concentration of NaCl additives in 0.2 M H_2SO_4 solution for 304 SS.

The effect of Cl^- and SO_4^{2-} on the anodic dissolution was investigated separately by Pyun et al. [30]. They observed pitting only in the presence of Cl^- and the adsorption of SO_4^{2-} ions does not cause pitting in all the applied anodic potential ranges. Thus, the additives of Cl^- ions accelerate the pitting corrosion of alloy in the H_2SO_4 solution [31]. Figure 2 shows the relationship between the pitting potential during potentiodynamic polarization and the chloride concentration in the H_2SO_4 solution for 304 SS. A high E_{pit} of 0.932 V was observed in the H_2SO_4 solution without chloride content, and only a slight reduction (−0.03 V) in the participation of 1 wt% NaCl additives. However, the value of E_{pit} decreased once the concentration of NaCl was increased over 1 wt%, and linear decrease of pitting potential was observed with the concentration of NaCl in the H_2SO_4 solution. When the concentration increased to 3 wt%, the value of pitting potential was dropped to 0.145 V, and pitting corrosion was more likely to occur. Therefore, the competition of SO_4^{2-} and Cl^- ions in potentiodynamic polarization behavior was demonstrated. In the low chloride-containing solution, SO_4^{2-} dominated the polarization, which resulted in a wide region of passivity and high value of E_{pit}. When the concentration of chloride increased, pitting potential rapidly decreased, and the results showed that the value of E_{pit} varied linearly with the concentration of NaCl additives in the H_2SO_4 solution.

3.2 Depth profile results

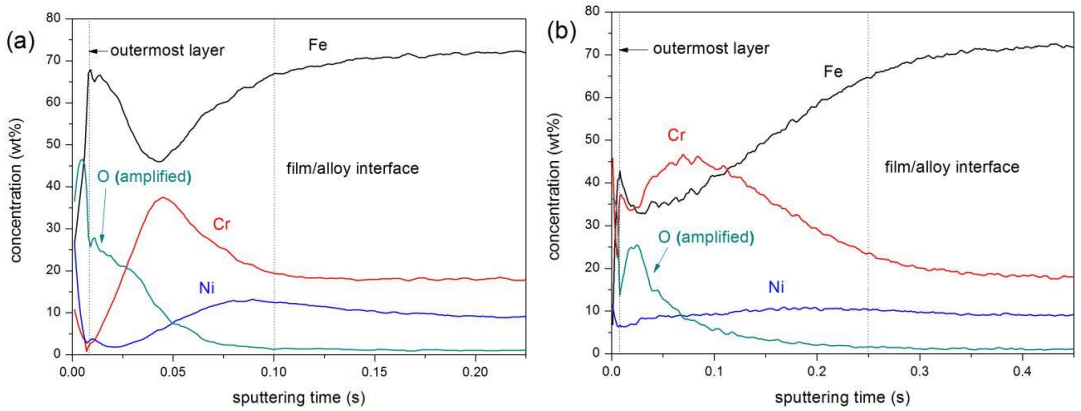

Figure 3. GD-OES depth profiles of passive film formed on 304 SS: (a) as-polished and (b) potentiostatic polarized in 0.2 M H_2SO_4 solution.

Glow discharge optical emission spectroscopy (GD-OES) depth profiles of the passive films formed on 304 SS during potentiostatic polarization in H_2SO_4 solution compared with as-polished specimen are shown in Figure 3. As main constituents in the passive film, four elements including Fe, Cr, Ni, and O were investigated. Irrational data were observed in the outermost layer and were regarded as unreliable because of surface contamination during handing of samples.

The enrichment of iron and chromium in the passive film was validated in many studies [32], but the concentration of Cr varied in different alloys and solution conditions. Abreu et al. [33] found that Cr oxide in the passive film of 316L SS decreased after eight potentiodynamic polarization cycles in 0.1 M NaOH solution. However, a Cr-enriched passive film was formed on 304 SS in aqueous solution according to Jung et al. [34]. The thickness of the passive film formed on the potentiostatic polarized specimen increased in comparison with the as-polished specimen as shown in Figure 3. The air-formed passive film consisted of two layers that are composed of an outer iron-rich and chromium- and iron-containing inner layers, which is in accordance with the GD-OES depth profiles investigated by Molchan et al. [35]. A large Fe species peak, as well as O species, were observed in the outer layer of air-formed passive film, which indicated the existence of iron oxide. Meanwhile, an increased amount of chromium and a reduced amount of iron appeared in the inner layer of the air-formed passive film. Ni species was nearly absent in the passive film of the specimen exposed to the air. A significant difference of polarized sample in Figure 3b is that a large amount of Cr was observed in the outer layer of the passive film, which led to the decrease of Fe in the region of passive film. More Ni species showed up in the passive film of polarized sample compared with the air-formed specimen.

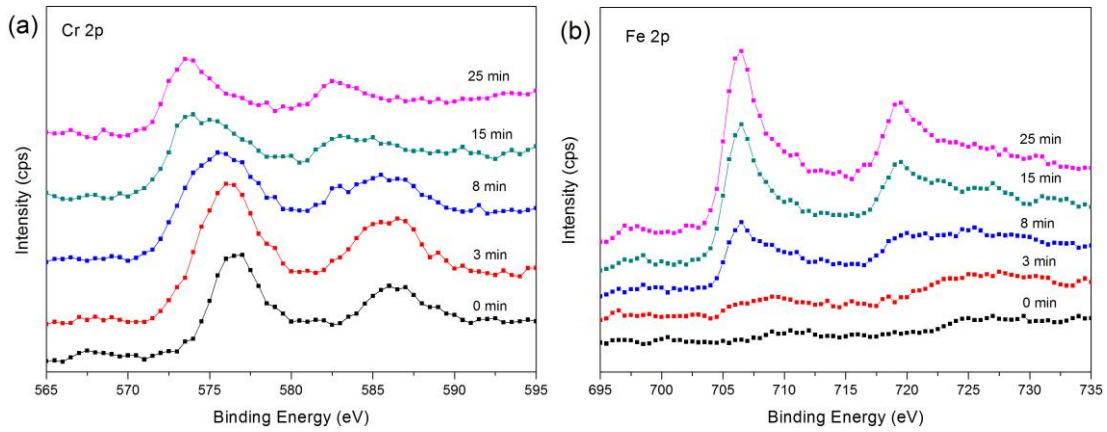

Figure 4. XPS spectra for (a) Cr 2p and (b) Fe 2p after different sputtering times (0, 3, 8, 15, and 25 min) of the passive film formed on 304 SS in 0.2 M H_2SO_4 solution.

Figure 4(a) shows XPS spectra of Cr 2p obtained from the surface of the passive film formed on 304 SS. Sputtering time corresponded to the depth of passive film from the outer layer to the alloy. The intensity of the peak increases with sputtering time up to 3 min, after which it started decreasing. A high-intensity peak at 576.5 eV±0.5 eV corresponded to 2p3/2, and a low-intensity peak at 586 eV± 0.5 eV to 2p1/2 were observed in the outer layer. This peak is possibly the supposed formation of chromium oxide such as Cr_2O_3. Leygraf et al. [36] found that chromium under all conditions is

enriched in the passivating film, and evidence for accumulation of chromium in their metallic state at the metal/passive film has been revealed under potentiostatic condition. The difference in binding energy between these two peaks was 9.7 eV, which was in good agreement with the standard value [37]. An evident change was observed in the peak position of the Cr 2p spectra with sputtering. The peak position shifted to 573.5 and 582.5 eV, which demonstrated the increase of Cr metal in the inner layer and substrate.

Fe 2p obtained from the surface of the passive film formed on the 304 SS (Figure 4(b)). A small amount of Fe species in the outer layer indicated that chromium oxide mainly constituted the great mass of the outer layer in the passive film. In the inner layer, a high-intensity peak at 706.5 eV±0.5 eV corresponded to 2p3/2 and a low-intensity peak at 719.5 eV± 0.5 eV to 2p1/2 suggested the existence of Fe metal, which is the most abundant material in the 304 SS. Appearance of a small peak in the inner layer of the passive film after 8 min of sputtering at 710.5 eV± 0.5 eV was attributed to Fe (III) oxide [16].

3.3 Effect of Cl^- ions

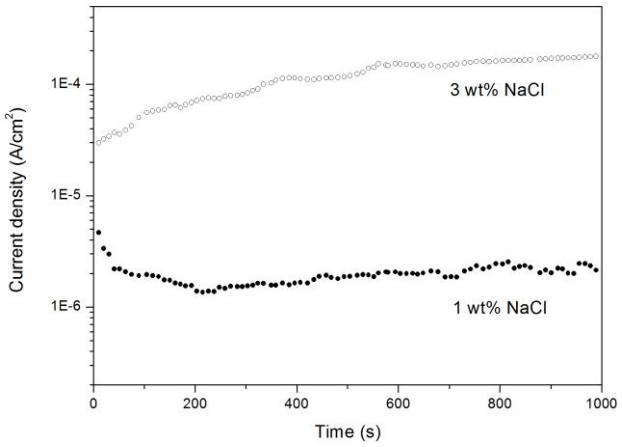

Figure 5. Variation of current density as a function of time for 304 SS exposed in 0.2 M H_2SO_4 containing 1 wt% and 3 wt% NaCl at 0.4 V (vs. SCE).

Figure 5 shows the variation of current density with immersion time of 304 SS in H_2SO_4 solution, which contains different concentrations of Cl^- ions. Gentle variation of the current density in 1 wt% NaCl-containing solution was observed with relatively low value of 1 to 2 μA/cm^2, which suggested that 304 SS specimens were still under the state of passivation. However, a substantial increase of current appeared when 3 wt% NaCl was added into H_2SO_4 solution, which indicated the occurrence of pitting corrosion caused by Cl^- ion additives. At the initial stage, the current density increased from the approximate value of 30 to 150 μA/cm^2, and the variation of current density with time flattened out.

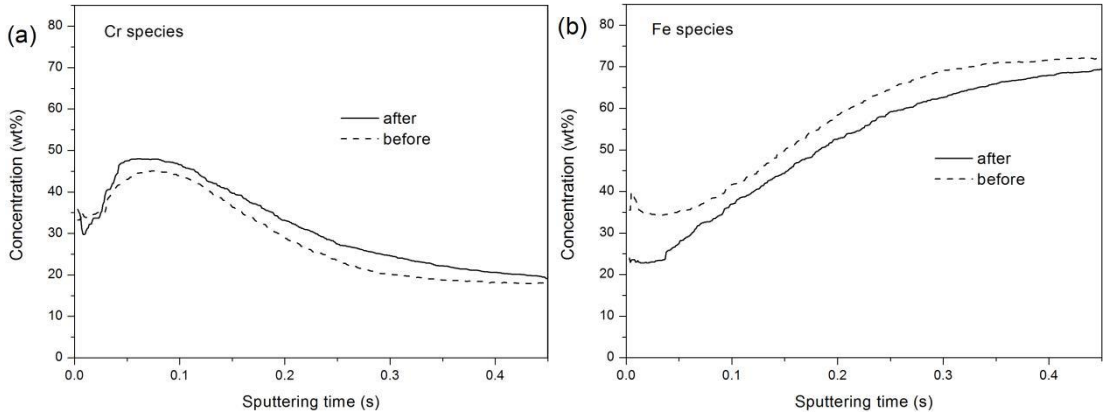

Figure 6. Variation of GD-OES elemental depth profiles of passive film of 304 SS after potentiostatic polarization in 0.2 M H_2SO_4 solution containing 1 wt% NaCl: (a) Cr species and (b) Fe species.

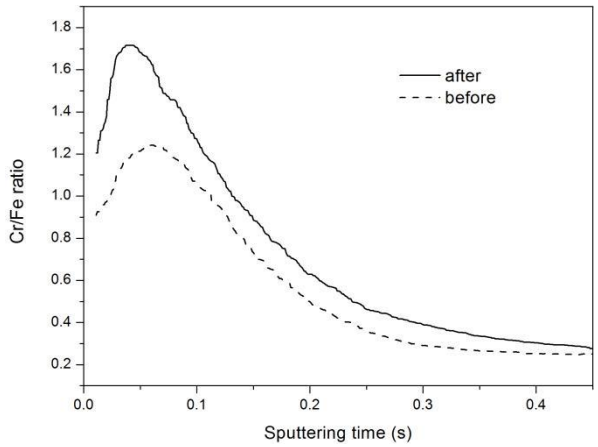

Figure 7. Variation of Cr/Fe ratio for passive film of 304 SS after potentiostatic polarization in 0.2 M H_2SO_4 solution containing 1 wt% NaCl.

The composition of the film depends on the condition of the formation, especially on the potential and the time of passivation [1]. Chloride ions promote the breakdown of the protective passive layer, thereby leading to the formation of corrosion pits [38]. Thus, the chemistry of passive film varied depending on the condition of surface reaction. Figure 6 shows the GD-OES elemental depth profiles of the passive film before and after potentiostatic polarization in H_2SO_4 solution that contains 1 wt% NaCl. Compared with the depth profiles of air-formed specimen in Figure 3(a), the concentration of chromium in passive film increased with the immersion time of potentiostatic passivation. The thickness of passive film also increased. As a result, the iron concentration decreased, especially in the outer layer of the passive film. As a critical factor to measure the corrosion resistance of the passive film, the Cr/Fe ratio of the passive film is described in Figure 7. The significant improvement in the Cr/Fe ratio in the region of the passive film was attributed to the increased thickness of the passive film after the potentiostatic passivation.

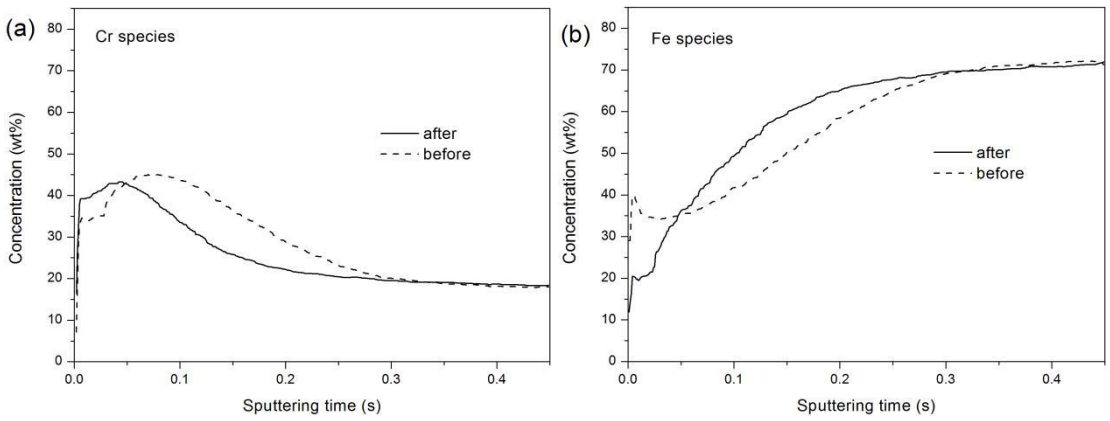

Figure 8. Variation of GD-OES depth profiles for the passive film of 304 SS after potentiostatic polarization in 0.2 M H_2SO_4 solution containing 3 wt% NaCl: (a) Cr species and (b) Fe species.

The GD-OES elemental depth profiles of the passive film before and after potentiostatic polarization in H_2SO_4 solution containing 3 wt% NaCl are shown in Figure 8. The rapid weight dropping of iron was observed on the surface of the passive film, which can be attributed to the dissolution of the iron-enriched outer layer during pitting corrosion. During the polarization, the surface film became thinner because of the pitting corrosion caused by Cl^- ions. The dissolution of the passive film in Cl^- ion-containing solution was attributed to the penetration of Cl^- ions through the passive film. Chloride is a relatively small anion with high diffusivity; thus, the soluble metal chloride takes the position of oxide in the passive film [39]. The presence of oxidizing agents in a chloride-containing environment is extremely detrimental and further intensifies localized corrosion.

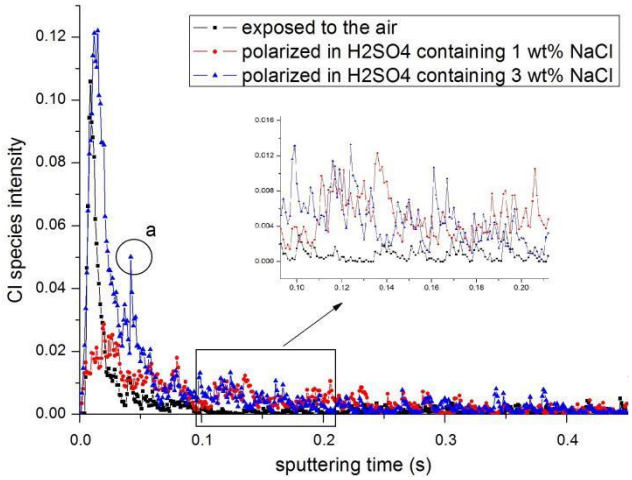

Figure 9. Chlorine species intensity for passive film of 304 SS in 0.2 M H_2SO_4 solution containing 1 and 3 wt% NaCl compared with that of air-formed passive film by GD-OES

The GD-OES depth profiles of chlorine species in the passive film of air-formed and polarized in H_2SO_4 solution containing different concentrations of NaCl are shown in Figure 9. The large peak of Cl species in the outermost region of the specimen exposed to the air was due to the chloride

contamination during handling of the specimens because Cl species was not supposed to be contained in the air-formed passive film. Chlorine is a common surface contamination that causes high chlorine ion yield [40].

The breakdown of passivity caused by chloride was revealed in the dissolution of oxide film, specifically iron and chromium oxide, which consisted of the chemistry of the passive film formed on 304 SS [41]. Three main mechanisms, namely, passive film penetration, film breaking, and adsorption, are discussed by Frankel [39]. Meng et. al [42] investigated the corrosion behavior of 316L stainless steel in chloride ions-containing solution. Their results indicated that the pitting corrosion of 316L stainless steel follows the adsorption mechanism in NaCl solution. Saadi et al. [17] studied the Cl^- ion concentration at the metal/film interface with an increase of the ending potential and found that Cl^- ions penetrate through the surface film and accumulated at the alloy/film interface.

As shown in Figure 9, a relatively small peak located in (a) was observed in the passive film region of the specimen polarized in H_2SO_4 solution containing 3 wt% NaCl, which indicated the enrichment of Cl species in the passive film if contamination was not considered. Moreover, the Cl species intensity decreased from the outer layer to the inner layer because of the penetration of Cl species through the passive film during pitting corrosion. Furthermore, chlorine was found in the passive film region of the 304 samples during potentiostatic passivation in H_2SO_4 solution containing 1 wt% NaCl. This condition suggested that Cl^- ions had an effect on the passive film despite undergoing passivation. At the near-alloy region (0.1–0.2 s in sputtering time relatively), a small amount of Cl species was also detected. The Cl^- intensity distribution obtained from the passive film region was in good agreement with the mechanisms of passive film penetration. The Cl^- ions in the solution penetrated from the outer layer to the inner layer with a decrease in content, which led to the dissolution of the passive film.

4. CONCLUSIONS

(1) The pitting potential of 304 SS during potentiodynamic polarization is related with the chloride concentration in H_2SO_4 solution. In the low chloride-containing solution, SO_4^{2-} dominated the polarization, which resulted in a broad passivation region and high value of E_{pit} (pitting potential). When the chloride concentration increased, the pitting potential rapidly decreased and the results showed that the value of E_{pit} varied linearly with the concentration of sodium chloride additives in the H_2SO_4 solution.

(2) A large amount of Cr species was observed in the passive film region of 304 SS during potentiostatic polarization in 0.2 M H_2SO_4 solution according to the GD-OES depth profiles, which was identified as Cr_2O_3 probably according to the X-ray photoelectron spectroscopy results. The Cr/Fe ratio increased with the immersion time of passivation, which indicated the improvement of corrosion resistance. The concentration of Fe species in the outer layer of the passive film decreased evidently as a result of pitting corrosion caused by chloride.

(3) The appearance of Cl species in the passive film region of 304 SS polarized in the chloride-containing solution suggested that Cl^- ions played an important role in polarization behavior. The

decrease of Cl species intensity from the outer layer to the inner layer validated the penetration of chloride ions through the passive film during pitting corrosion.

ACKNOWLEDGMENTS
This work was supported by the Fundamental Research Funds for the Central Universities (HUST: 2011TS119) in China. The authors are grateful to HORIBA Jobin Yvon for the help in carrying out the GDOES profiles. A special thank is given to HUST Analytical & Testing Center for XPS analysis.

References

1. G. Okamoto, *Corros. Sci.*, 13 (1973) 471.
2. K. Varga, E. Maleczki, *Electrochim. Acta*, 33 (1988) 1775.
3. K. Varga, E. Maleczki, *Electrochim. Acta*, 33 (1988) 25.
4. W. Tian, N. Du, S. Li, S. Chen, Q. Wu, *Corros. Sci.*, 85 (2014).
5. C.B. Santos, M. Metzner. C.F. Malfatti, J.Z. Ferreira, *Electrochim. Acta*, 120 (2014) 284.
6. J. Wu, X. Li. C. Du, S. Wang, Y. Song, *J. Mater. Sci. Technol.*, 21 (2005) 28.
7. S. Ericson, J. Kurol, *Int. J. Electrochem. Sci.*, 8 (2013) 5851.
8. J.A. Cabral-Miramontes, J.D. O.Barceinas-Sánchez. C.A. Poblano-Salas, G.K. Pedraza-Basulto, D. Nieves-Mendoza, P. C. Zambrano-Robledo, F. Almeraya-Calderón , J. G. Chacón-Nava, *Int. J. Electrochem. Sci.*, 8 (2013) 564.
9. M. Saadawy, *Int. J. Electrochem. Sci.*, 11 (2016) 2345.
10. R.T. Loto, *J. Mater. Environ. Sci.*, 4 (2013) 448.
11. W.J. Lee, S.I. Pyun. *Electrochim. Acta*, 45 (2000) 1901.
12. Y. Yi, P. Cho, A. Al Zaabi, Y. Addad, C. Jang, *Corros. Sci.*, 74 (2013) 92.
13. L. Guan, B. Zhang, X.P. Yong, J.Q. Wang, E.H. Han, W. Ke, *Corros. Sci.*, 93 (2015) 80.
14. S. Réguer, P.Dillmann, F. Mirambet, *Corros. Sci.*, 49 (2007) 2726.
15. M. Janik-Czachor, S. Kaszczyszyn, *Mater. Corros*, 33 (1982) 500.
16. V.S. Rao, L.K. Singhal, *J. Mater. Sci.*, 44 (2009) 2327.
17. S. A. Saadi, Y. Yi, P. Cho, C. Jang, P. Beeley, *Corros. Sci.*, 111 (2016) 720.
18. D.G. Li, J.D.Wang, D.R. Chen, *Int. J. Hydrogen Energ.*, 39 (2014) 20105.
19. Z. Qin, X. Pang, L. Qiao, M. Khodayari, A. A. Volinsky, *Appl. Surf. Sci.*, 303 (2014) 282.
20. H. Luo, S.Gao, C. Dong, X. Li, *Electrochim. Acta*, 135 (2014) 412.
21. S. Mischler, H.J. Mathieu, D. Landolt, *Surf. Interface Anal.*, 11 (1988) 182.
22. K. Rokosz, J. Labtinen, T. Hryniewicz, S. Rzadkiewicz, *Surf. Coat. Tech.*, 276 (2015) 516.
23. M. Uemura, T. Yamamoto, K. Fushimi, Y. Aoki, K. Shimizu, H. Habazaki, *Corros. Sci.*, 51 (2009) 1554.
24. Y. Liu, W.Jian, J.Y. Wang, S. Hofmann, K. Shimizu, *Appl. Surf. Sci.*, 331 (2015).
25. M. Dumerval, S. Perrin, L. Marchetti, M. Tabarant, F. Jomard, Y. Wouters, *Corros. Sci.*, 85 (2014) 251.
26. I. Nakatsugawa, K. Araki, H. Takayasu, K. Saito, K. Matsusaka, T. Endou, A. Shida, *Surf. Coat. Tech.*, 169 (2003) 307.
27. S. Hofmann, Y. Liu, J.Y. Wang, J. Kovac, *Appl. Surf. Sci.*, 314 (2014) 942.
28. Z.B. Zheng, Y.G. Zheng, *Corros. Sci.*, 112 (2016) 657.
29. X.L. Zhang, Zh.H. Jiang, Zh.P. Yao, Y. Song, Zh.D. Wu, *Corros. Sci.*, 51(2009)581
30. S.I. Pyun, SM. Moon, S.H. Ahn, S.S. Kim, *Corros. Sci.*, 41(1999)653.
31. T. Hong, M. Nagumo, *Corros. Sci.*, 39 (1997) 961-967.
32. P. Brüesch, K. Müller, A. Atrens, H. Neff, *Phys. A*, 38(1985)1.
33. C.M. Abreu, M.J. Cristóbal, R. Losada, X.R. Nóvoa, G. Pena, M.C. Pérez, *J. Electroanal. Chem.*, 572(2004)335.

34. R.H. Jung, H. Tsuchiya, S. Fujimoto, *Corros. Sci.*,58(2012)62.
35. I.S. Molchan, G.E. Thompson, J. Walton, P. Skeldon, A. Tempez, S. Legendre, *Appl. Surf. Sci.*, 357 (2015) 37.
36. C. Leygraf, G. Hultquist, I. Olefjord, B.-O. Elfström, V.M. Knyazheva, A.V. Plaskeyev, Ya.M. Kolotyrkin, *Corros. Sci.*, 19(1979)343.
37. C.D. Wagner, W.M. Riggs, L.E. Davis, J.F. Moulder, G.E. Muilenberg, Handbook of X-ray photoelectron spectroscopy. PerkinElmer Corporation, (1979) Minnesota.
38. M.Shabani-Nooshabadi, M.S. Ghandchi, *J. Ind. Eng. Chem.*, 31(2015)231.
39. G.S. Frankel, *J. Electrochem. Soc.*, 145 (1998) 2186.
40. K.A. Arushanov, M.N. Drozdov, S.M. Karabanov, I.A. Zeltser, A. Tolstogouzov, *Appl. Surf. Sci.*, 265 (2013) 642.
41. M.E. Curley-Fiorino, G.M. Schmid, *Corros. Sci.*, 20(1980)313.
42. G. Meng, Y. Li, Y. Shao, T. Zhang, Y. Wang, F.Wang, *J. Mater. Sci. Technol.*, 30(2014)253.